Wave-particle resonance and gyrobunching in the lower hybrid drift instability

J W S Cook[1], R O Dendy[2,1] and S C Chapman[1]

[1]*Centre for Fusion, Space and Astrophysics, Department of Physics, Warwick University, Coventry CV4 7AL, U.K.*

[2]*Euratom/CCFE Fusion Association, Culham Science Centre, Abingdon, Oxfordshire OX14 3DB, U.K.*

We study the physics of the excitation mechanism of the lower hybrid drift instability (LHDI), using a 1D3V particle-in-cell (PIC) code (epoch1d, based on Ref. [1]) which provides a fully kinetic description of the interaction between minority ($\sim 1\%$) 3MeV protons, majority thermal deuterons, electrons, the self-consistent electromagnetic fields, and the imposed background magnetic field. The background magnetic field is oriented at 84° to the single spatial domain x. We focus on the particle dynamics which exhibit coherent bunching that is structured in velocity space and real space. The LHDI [2] is potentially operative wherever drifting populations of ions occur in magnetised plasmas. In this case the instability arises due to the ring-beam (in velocity space) character of the fast ion population. See Refs. [3–5] for details relating to ring-beam fast ions interactions with fast Alfvén waves that are responsible for ion cyclotron emission. Predominantly electrostatic waves, propagating quasi-perpendicular to the magnetic field, are preferentially excited with a frequency that is characterised by the lower hybrid frequency $\omega_{LH} = \Omega_{ce}\Omega_{ci}/(1+\Omega_{ce}\Omega_{ci}/\omega_{pi}^2)$. In Refs. [6, 7] it was shown that ring-beam distributions, i.e. $f(v_\perp, v_\parallel) = 1/(2\pi v_r)\delta(v_\perp - v_r)\delta(v_\parallel - u)$, can also be unstable against the LHDI.

Figure 1 shows a single proton's motion through configuration space x and gyrophase $\alpha = \arctan(v_{\perp,1}/v_{\perp,2})$ for one unperturbed cyclotron orbit. The shading (colour online) of the trace in Fig 1a represents time, while in Fig 1b shading (colour online) represents velocity v_x.

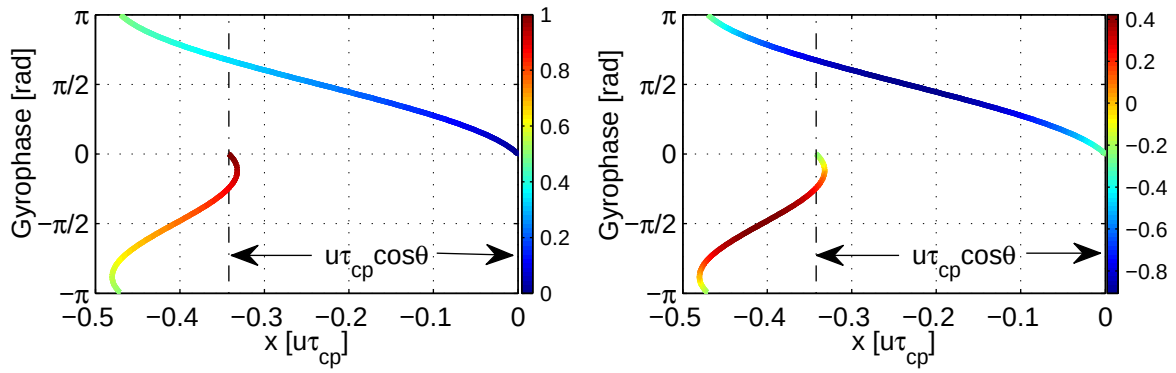

(a) (b)

Figure 1: (Reproduced from [8]).

It is known that, for the simulations parameters of Figs.3 and 4 of Ref. [6], the dominant collectively excited modes propagate in the negative x-direction with slightly lower phase speed than the maximum negative proton speed. Modes with lower amplitudes are excited propagating with similar phase speeds in both directions along x, near the maxima of transient speeds of the energetic protons that drive the instability. These maxima of occur (see Fig. 1) at gyrophases $\alpha = \pm\pi/2$; see also panel (a) of Fig.2 of Ref. [7].

Figure 2a plots the electron distribution at a snapshot in time towards the end of the linear stage of the instability. It confirms that the predominantly electrostatic wave is supported by an electron density oscillation. The full simulation domain accommodates 21 wavelengths of this lower hybrid wave, of which 10.5 are plotted in the half-box of Fig 2 for reasons of pictorial resolution (ditto Fig. 3). The resonant interaction between the protons and the wave is visible in the distribution of proton energies, shown in Fig. 2b. The strong spatially dispersive distortion at $\alpha = \pi/2$ corresponds (see Fig.1) to the maximum negative particle velocity (see also Fig.2(a) of Ref. [7]), which is located between the points in gyrophase where the resonant drive of the dominant backward-propagating waves takes place. Resonant interactions condition the long-wavelength (in gyrophase α) energy structure across the positive-α domain of phase space. At $\alpha = -\pi/2$, which corresponds to the maximum positive particle velocity, the consequences of resonance with a less powerful wave are apparent in the Moiré pattern.

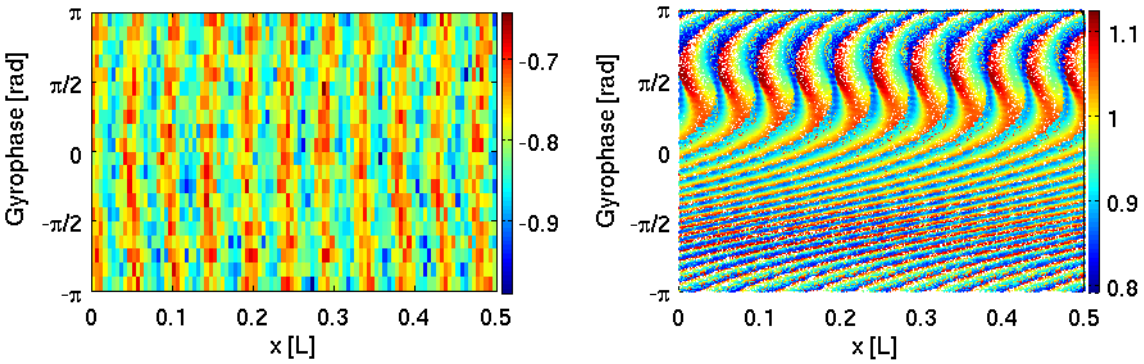

(a) (b)

Figure 2: PIC code derived particle population data from a time snapshot towards the end of the linear stage of the instability, plotted in (α, x)-space. Panel (a): Electron probability density on a log_{10} scale indicated by shading (colour online). Panel (b): Proton energy, in units of the initial proton energy, indicated by shading (colour online). 10.5 nearly-identical s-shaped features appear in the upper half plane at regular spatial intervals, as well a Moiré pattern in the lower half (Reproduced from [8]).

Figure 3 is constructed on the basis that the value of the field amplitude $\mathscr{E}$, experienced by the particle at the point of resonance, is a good proxy for the strength of the interaction. At each (α, x), Fig. 3 plots $\mathscr{E}$, inferred using the analytical model of Eqns. (12) to (16) of Ref. 7, at the time where the particle was last in resonance. Figure 3a plots $\mathscr{E}$ for energetic protons subjected to the dominant wave. Figure 3b is derived for the sum of three waves: the dominant wave, of unit amplitude; its harmonic, of 1/10 amplitude; and a forward travelling wave, of 1/4 amplitude, where PIC simulations provide the waves' spectral data.

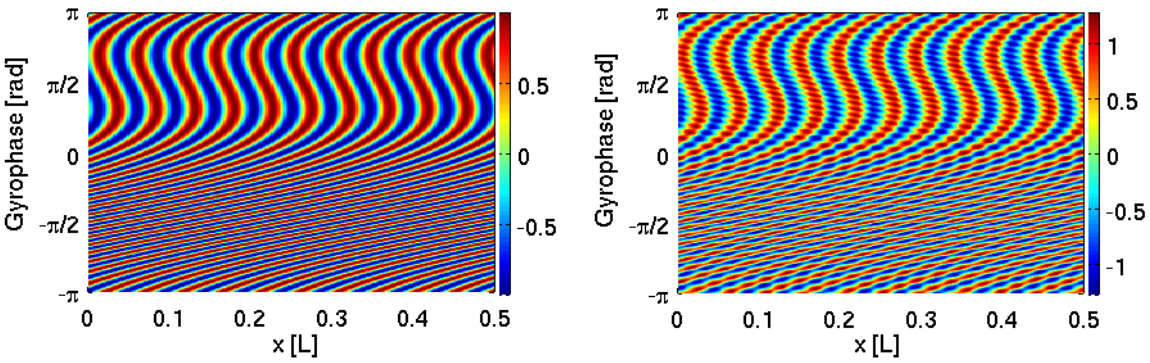

(a) (b)

Figure 3: Normalized electric field amplitude $\mathscr{E}$ indicated by shading (colour online) experienced by protons at their most recent resonance at a snapshot in time. Panel (a) - dominant wave. Panel (b) - 3 most powerful waves (Reproduced from [8]).

Figure 3b captures the key features of Fig. 2b, suggesting that the analytical model recreates gyrobunching effects seen in the PIC simulations. This is the case because the perturbations are such that the resonant gyrophase angles are sharply defined, and the spatial deviation (as distinct from gyrophase deviation) of the resonant particles from their unperturbed orbits is small compared to the wavelength of the excited waves. Our results thereby capture the key physics of the lower hybrid drift instability, which is a beam-type resonance that is localised to a short angular segment of the ion gyro-orbit.

This work was part-funded by the RCUK Energy Programme under grant EP/I501045 and the European Communities under the contract of Association between EURATOM and CCFE. The views and opinions expressed herein do not necessarily reflect those of the European Commission.

References

[1] M. Bonitz, G. Bertsch, V. S. Filinov, and H.Ruhl. *Introduction to Computational Methods in Many Body Physics*. Cambridge University Press, Cambridge, 2004.

[2] O. J. G. Silveira, L. F. Ziebell, R. Gaelzer, and P. H. Yoon. Unified formulation for inhomogeneity-driven instabilities in the lower-hybrid range. *Phys. Rev. E*, 65(3):036407, Feb 2002.

[3] G. A. Cottrell and R. O. Dendy. Superthermal radiation from fusion products in JET. *Phys. Rev. Lett.*, 60(1):33–36, Jan 1988.

[4] R. O. Dendy, K. G. McClements, C. N. Lashmore-Davies, G. A. Cottrell, R. Majeski, and S. Cauffman. Ion cyclotron emission due to collective instability of fusion products and beam ions in TFTR and JET. *Nuclear Fusion*, 35:1733–1742, Dec 1995.

[5] S. Cauffman, R. Majeski, K. G. McClements, and R. O. Dendy. Alfvénic behaviour of alpha particle driven ion cyclotron emission in TFTR. *Nuclear Fusion*, 35(12):1597–602, 1995.

[6] J. W. S. Cook, S. C. Chapman, and R. O. Dendy. Electron current drive by fusion-product-excited lower hybrid drift instability. *Phys. Rev. Lett.*, 105(25):255003, Dec 2010.

[7] J W S Cook, S C Chapman, R O Dendy, and C S Brady. Self-consistent kinetic simulations of lower hybrid drift instability resulting in electron current driven by fusion products in tokamak plasmas. *Plasma Physics and Controlled Fusion*, 53(6):065006, 2011.

[8] J. W. S. Cook, R. O. Dendy, and S. C. Chapman. Gyrobunching and wave-particle resonance in the lower hybrid drift instability. *Plasma Physics and Controlled Fusion*, 53(7):074019, 2011.